

Origin of the blueshift in the intersubband infrared absorption in GaAs/Al_{0.3}Ga_{0.7}As multiple quantum wells

M. O. Manasreh

Electronic Technology Directorate (WL/ELRA), Wright Laboratory, Wright-Patterson Air Force Base, Ohio 45433-6543

F. Szmulowicz and T. Vaughan

University of Dayton Research Institute, 300 College Park Avenue, Dayton, Ohio 45469

K. R. Evans and C. E. Stutz

Electronic Technology Directorate (WL/ELRA), Wright Laboratory, Wright-Patterson Air Force Base, Ohio 45433-6543

D. W. Fischer

Materials Directorate (WL/MLPO), Wright Laboratory, Wright-Patterson Air Force Base, Ohio 45433-6533

(Received 18 January 1991)

The intersubband transition (IT) in GaAs/Al_{0.3}Ga_{0.7}As multiple-quantum-well samples measured by the infrared-absorption technique at 5 K is studied as a function of the two-dimensional electron-gas density (σ). A blueshift in the peak-position energy of the IT is observed as σ increases. Single-particle calculations of the optical-absorption spectra, which are obtained by using the nonparabolic-anisotropic envelope-function approximation (EFA), indicate that the peak-position energy should show a redshift as σ is increased. We found that it is necessary to incorporate many-body corrections (in particular electron-electron intrasubband exchange and direct Coulomb interaction energies), depolarization, and excitonlike shifts in the EFA calculations in order to account for the experimental peak-position energy and blueshift as σ is increased.

Intersubband transitions (IT's) in III-V semiconductor multiple quantum wells (MQW's) have been the subject of numerous studies in recent years. These transitions reveal behaviors due to the presence of fundamental features, such as electron-electron interactions,¹ depolarization,²⁻⁴ and reduced dimensionality.⁵ In addition, long-wavelength detectors⁶ and optical modulators^{7,8} have motivated the study of these transitions. It was demonstrated⁹ that the oscillator strength of such transitions is very large in GaAs/Al_xGa_{1-x}As MQW's. One important aspect of these transitions in systems such as GaAs/Al_xGa_{1-x}As MQW (Ref. 10) and In_xGa_{1-x}As/Al_xGa_{1-x}As MQW (Ref. 11) is the observation of a blueshift in their peak-position energy (PPE) as the temperature is decreased (we will refer to this shift as temperature blueshift). It was concluded that the nonparabolicity alone cannot explain the temperature blueshift observed in barrier-doped materials.¹⁰ A second type of blueshift in PPE is also observed as the two-dimensional electron-gas (2DEG) density (σ) in GaAs/Al_xGa_{1-x}As MQW's (Refs. 2 and 3) and In_xGa_{1-x}As/Al_xGa_{1-x}As MQW's (Ref. 12) is increased (we will refer to this shift as density blueshift). Ramsteiner *et al.*³ and Dischler *et al.*¹³ interpreted the density blueshift as being due to the depolarization and band-filling effects alone. On the other hand, Pinczuk *et al.*² proposed that this type of blueshift is resulting from the direct and exchange intersubband Coulomb interactions.

In this Rapid Communication, we will show that the density blueshift of PPE observed in GaAs/Al_xGa_{1-x}As MQW samples at low temperatures as σ is increased can be quantitatively accounted for when the depolarization

effect, electron-electron exchange, and direct Coulomb interactions for the ground state, and excitonlike effect are incorporated in the nonparabolic-anisotropic envelope-function approximation. On the other hand, the results of single-particle calculations exhibit a redshift as a function of σ .

The samples were grown on semi-insulating GaAs substrates by molecular-beam epitaxy (MBE) and consisted of a 1000-Å undoped GaAs buffer layer followed by 100 periods of 75-Å silicon-doped GaAs quantum wells and 100-Å undoped Al_{0.3}Ga_{0.7}As barriers. This was followed by a 75-Å undoped GaAs cap layer. An additional barrier-doped sample that was used previously¹⁰ is also included in the current investigation. The infrared absorption was recorded at the Brewster's angle of GaAs ($\sim 73^\circ$) from the normal using a Bomem DA3 Fourier-transform interferometer. The samples were cooled to 5 K using a continuous flow cryostat and the temperature was controlled within ± 0.5 K.

Typical intersubband absorption spectra are shown in Fig. 1 for 5 different samples with different dopant concentrations. The spectrum labeled curve *a* is obtained for the barrier-doped sample. It is clear from this figure that the peak-position energy is increased (blueshift) as σ is increased. In order to analyze the density blueshift, the total integrated absorption (*I*) of the IT spectrum of each sample is converted to the 2DEG density, σ , according to the relationship⁹

$$I \approx \frac{N\sigma L e^2 h}{4\epsilon_0 m^* c} \frac{f}{n^2(n^2+1)^{1/2}},$$

where *N* is the number of wells, *L* is the well width (75

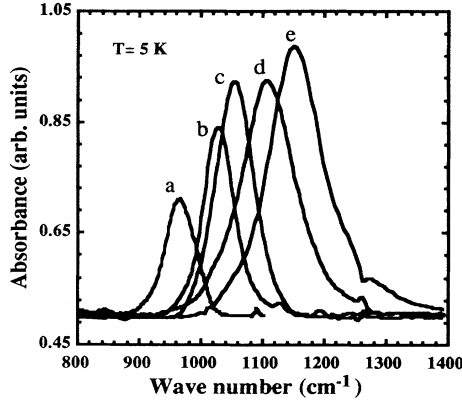


FIG. 1. Selected intersubband infrared absorption spectra in GaAs/Al_{0.3}Ga_{0.7}As MQW's with different dopant concentrations (σ). Curves *a*, $3.25 \times 10^{11} \text{ cm}^{-2}$; *b*, $1.09 \times 10^{12} \text{ cm}^{-2}$; *c*, $1.13 \times 10^{12} \text{ cm}^{-2}$; *d*, $1.80 \times 10^{12} \text{ cm}^{-2}$; and *e*, $2.29 \times 10^{12} \text{ cm}^{-2}$. All samples were doped in the well except curve *a* which was doped in the barrier.

\AA), m^* is the electron effective mass in GaAs, n is the refractive index of GaAs (~ 3.3), and f is the oscillator strength (~ 13.91 for the present MQW). The results are shown in Fig. 2 as solid squares. The vertical error bars were introduced to account for a monolayer inhomogeneity in the GaAs quantum well across the sample.

In order to estimate the peak-position energies of the intersubband transition spectra, the linear absorption coefficient $\alpha(\nu)$ is first calculated from the following expression:

$$\alpha(\nu) \sim (1/\nu) \int d^2\mathbf{k} |\mathbf{M}|^2 \delta(E_1 - E_0 - h\nu) \times f(E_0) [1 - f(E_1)], \quad (1)$$

where the integral is over the Brillouin zone, E_0 and E_1 are the ground and excited state energies as a function of wave vector in the plane of the well, $|\mathbf{M}|^2$ is the oscillator strength, and $f(E_i)$ are the Fermi-Dirac distribution functions. The energies, E_0 and E_1 , were calculated using single-particle band structure for the well as a function of the wave vector following Ekenberg's nonparabolic-anisotropic envelope function formalism.¹⁴ In these calculations, the effective masses of both the well and the barrier were obtained from their dependence on the band gap¹⁵ which was calculated using Varshni parametrization¹⁶ and the conduction-to-valence-band offset ratio was taken¹⁷ as $\frac{57}{43}$. The IT peak position energy (we will refer to the theoretical peak-position energy as $h\nu_0$) is then obtained from the broadened $\alpha(\nu)$, $\bar{\alpha}(\nu)$, using a Lorentzian line shape and is given by

$$\bar{\alpha}(\nu) = \int (1/\pi) \frac{\Gamma_0}{\Gamma_0^2 + (\nu - \nu')^2} \alpha(\nu') d\nu', \quad (2)$$

where $\alpha(\nu')$ is the same as Eq. (1); and $\Gamma_0 = \gamma_1 + \gamma_2 / [\exp(\hbar\omega/kT) - 1]$, where γ_1 and γ_2 are constants and $\hbar\omega$ is the longitudinal phonon mode of GaAs (for further details see Ref. 10). The result of $h\nu_0$ as a function of σ is shown in Fig. 2 as the short-dashed line. The latter results exhibit a redshift as σ is increased which is in

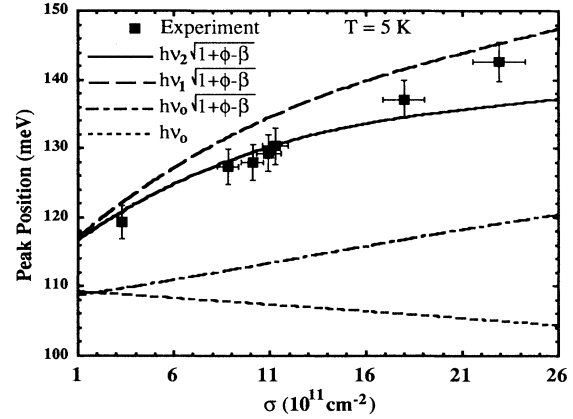


FIG. 2. The peak-position energy of the intersubband transition as a function of σ . The closed squares represent the experimental data, the short-dashed line represents the single-particle calculations of the intersubband transition energy, i.e., $h\nu_0$, the long-short-dashed line represents Eq. (3) which includes the depolarization and excitonlike effects, the long-dashed line represents Eq. (3) with $h\nu_0$ replaced by $h\nu_1$ which includes the exchange interaction effect in addition to the depolarization and excitonlike effects, and the solid line represents Eq. (3) with $h\nu_0$ replaced by Eq. (8) which includes the direct Coulomb interaction effect in addition to the depolarization, excitonlike, and exchange interaction effects.

disagreement with the experimental measurements. However, the behavior of $h\nu_0$ as a function of σ is in good agreement with the depolarized-light Raman scattering measurements of single-particle transitions.³

The next step is to investigate the depolarization (plasmon shift) and excitonlike (interaction of the excited electron with the hole in the ground state, analogous to the exciton associated with the valence-to-conduction-band transition) effects on $h\nu_0$. In order to include these effects we used the formalism of Ando,¹⁸ which gives the shifted intersubband transition energy (ΔE) as

$$\Delta E = h\nu_0 \sqrt{1 + \phi - \beta}, \quad (3)$$

where the factor ϕ accounts for the depolarization shift and is given by

$$\phi = 2 \frac{4\pi e^2}{\epsilon} \sigma S_{01} \frac{1}{h\nu_0}, \quad (4)$$

where ϵ is the dielectric constant and S_{01} is the Coulomb matrix element given by

$$S_{01} = \int_0^\infty dz \left[\int_0^z \xi_1(z') \xi_0(z') dz' \right]^2, \quad (5)$$

where ξ_0 and ξ_1 are the wave functions for the ground and excited states, respectively. The factor β in Eq. (3) accounts for the excitonlike shift given by

$$\beta = - \frac{2\sigma}{h\nu_0} \int_{-\infty}^{+\infty} dz \xi_1(z)^2 \xi_0(z)^2 \frac{\partial V_{xc}(\sigma(z))}{\partial \sigma(z)}, \quad (6)$$

where $V_{xc}(\sigma(z))$ is the exchange-correlation potential as a function of the local sheet density $\sigma(z)$ and is described elsewhere.¹⁹ The result of Eq. (3) after calculating Eqs.

(4)–(6) is presented in Fig. 2 as the long-short-dashed line. Three points should be mentioned here. First, the excitonlike shift is very small as compared to the depolarization shift. Second, Eq. (3) produces a trend similar to that of the experimental data, i.e., a blueshift as σ is increased. Third, the experimental peak-position energy as a function of σ is much larger than the results obtained from Eq. (3). Thus, the depolarization and excitonlike shifts alone do not appear to account for what is observed experimentally and, therefore, other effects should be considered.

Since the dopant densities in the present MQW samples are relatively high, one would expect that many-body effects such as electron-electron exchange and direct Coulomb interactions for the ground state are significant. Bandara *et al.*¹ derived approximate expressions for these interactions and concluded that the electron-electron exchange interaction energy for the ground state ($E_{\text{exch}}(k)$) is sizable and given by

$$E_{\text{exch}}(k) \approx \frac{-e^2 k_F}{4\pi\epsilon} \left[\frac{2E(k/k_F)}{\pi} - 0.25 \frac{k_F}{k_L} \right], \quad (7)$$

where $k_F = \sqrt{2\pi\sigma}$, $k_L = \pi/L$, and $E(k/k_F)$ is a complete elliptic integral. By adding $E_{\text{exch}}(k)$ to the ground-state energy E_0 in Eq. (1), one can obtain the peak-position energy of the IT which is defined here as $h\nu_1$. The results of Eq. (3) after replacing $h\nu_0$ in Eqs. (3), (4), and (6) by $h\nu_1$ using Eq. (7) are presented by the long-dashed line in Fig. 2. Thus far, it is evident that the agreement between theory and experiment is greatly improved by including depolarization, excitonlike, and exchange interaction effects. It should be pointed out that the exchange interaction alone when it is added to the single-particle calculations cannot explain the peak position as a function of σ . The agreement between theory and experiment can be further improved by replacing $h\nu_0$ in Eqs. (3), (4), and (6) with

$$h\nu_2 = h\nu_1 - E_{\text{dir}}, \quad (8)$$

where the direct Coulomb interaction energy for the ground state, E_{dir} , derived for an electrically neutral doped well is given by¹

$$E_{\text{dir}} = \frac{3\sigma e^2}{8\epsilon k_L^2 L}. \quad (9)$$

The peak-position energies obtained from Eq. (3) using Eqs. (8) and (9) are shown as the solid line in Fig. 2. From this figure, the effect of E_{dir} term on ΔE is small (~ 1 meV at $3 \times 10^{11} \text{ cm}^{-2}$) as compared to that of E_{exch} or the depolarization shift, and becomes considerably larger as σ is increased (~ 10 meV at $2.6 \times 10^{12} \text{ cm}^{-2}$). The agreement between experiment and theory when the depolarization shift, excitonlike shift, exchange interaction energy, and direct Coulomb interaction energy are included is remarkable, in particular for $\sigma \leq 16 \times 10^{11} \text{ cm}^{-2}$. On the other hand, these effects cannot account for the experimental peak-position energy of the IT as a function of σ when they are considered separately. For $\sigma \geq 16 \times 10^{11} \text{ cm}^{-2}$ the agreement between theory (solid line) and experiment (closed squares) in Fig. 2 is not admirable. In addition, the temperature blueshift obtained experimentally from the difference between peak positions recorded at 5 and 300 K is found to increase approximately linearly with σ while our calculations using Eqs. (3) and (8) show an opposite trend (decrease as a function of σ) when the temperature variation is included. Further analysis regarding this discrepancy will be discussed in a separate article.

In conclusion, we have shown that the blueshift observed in the peak-position energy of the intersubband transition in GaAs/Al_xGa_{1-x}As MQW's at 5 K as a function of the 2DEG density, σ , is quantitatively accounted for when the depolarization, excitonlike, the ground-state electron-electron exchange interaction, and the ground-state direct Coulomb interaction effects are incorporated in the nonparabolic-anisotropic envelope function approximation calculations. All these effects are found to be necessary in order to account for what is observed experimentally. Single-particle calculations, on the other hand, show a redshift as a function of σ in good agreement with Raman scattering measurements.³ Further analysis is required in order to explain the increase of the temperature blueshift as σ is increased.

This work was partially supported by the Air Force Office of Scientific Research. F. Szmulowicz and T. Vaughan were supported under U.S. Air Force Contract No. F33615-88-C-5423. We would like to thank E. Taylor and J. Ehret for the MBE growth.

- ¹K. M. S. V. Bandara, D. D. Coon, O. Byungsung, Y. F. Lin, and M. H. Francombe, *Appl. Phys. Lett.* **53**, 1931 (1988).
²A. Pinczuk, S. Schmitt-Rink, G. Danan, J. P. Valladares, L. N. Pfeiffer, and K. W. West, *Phys. Rev. Lett.* **63**, 1633 (1989).
³M. Ramsteiner, J. D. Ralston, P. Koidl, B. Dischler, H. Beibl, J. Wagner, and H. Ennen, *J. Appl. Phys.* **67**, 3900 (1990).
⁴A. Pinczuk and G. Abstreiter in *Light Scattering in Solids V*, edited by M. Cordona and G. Güntherodt (Springer-Verlag, New York, 1989), p. 153.
⁵T. Ando, A. B. Fowler, and F. Stern, *Rev. Mod. Phys.* **54**, 437 (1982).
⁶B. F. Levine, C. G. Bethea, G. Hasnain, J. Walker, and R. J. Malik, *Appl. Phys. Lett.* **53**, 296 (1988); B. F. Levine, K. K.

- Choi, C. G. Bethea, J. Walker, and R. J. Malik, *ibid.* **50**, 1092 (1987).
⁷A. Harwit and J. S. Harris, Jr., *Appl. Phys. Lett.* **50**, 685 (1987).
⁸N. F. Johnson, H. Ehrenreich, and R. V. Jones, *Appl. Phys. Lett.* **53**, 180 (1988).
⁹L. C. West and S. J. Eglash, *Appl. Phys. Lett.* **46**, 1156 (1985).
¹⁰M. O. Manasreh, F. Szmulowicz, D. W. Fischer, K. R. Evans, and C. E. Stutz, *Appl. Phys. Lett.* **57**, 1790 (1990); F. Szmulowicz, M. O. Manasreh, D. W. Fischer, F. Madarasz, K. R. Evans, E. Stutz, and T. Vaughan, *Superlattices Microstruct.* **8**, 63 (1990).
¹¹X. Zhou, P. K. Bhattacharya, G. Hugo, S. C. Hong, and E.

- Gulari, Appl. Phys. Lett. **54**, 855 (1989).
- ¹²Y. Shakuda and H. Katahama, Jpn. J. Appl. Phys. **29**, L552 (1990).
- ¹³B. Dischler, J. D. Ralston, P. Koidl, P. Hiesinger, M. Ramsteiner, and M. Maier, in *Long-Wavelength Semiconductor Devices, Materials and Processes*, edited by A. Katz, R. M. Biefeld, R. J. Malik, and R. L. Gunsher (Materials Research Society, Pittsburgh, to be published).
- ¹⁴U. Ekenberg, Phys. Rev. B **36**, 6152 (1987).
- ¹⁵J. S. Blakemore, J. Appl. Phys. **53**, R123 (1982).
- ¹⁶Y. P. Varshni, Physica **34**, 149 (1967).
- ¹⁷S. Adachi, J. Appl. Phys. **58**, R1 (1985).
- ¹⁸T. Ando, Solid State Commun. **21**, 133 (1977).
- ¹⁹W. L. Bloss, J. Appl. Phys. **66**, 3639 (1989).